Quantitative Study on 2D Spatial Autocorrelation in Intrinsic Imaging of Optical Signals

Authors: Mei Duanmu, Jingran Li, Dong Yan

Advisors: Haley Hedlin, Daryl Hochman, John Staudenmayer

1. Introduction

Approximately 2 million people in the US have epilepsy, and 20%-30% of the population has epilepsy refractory to all forms of medical treatment. The best viable treatment for patients with medically intractable epilepsy is the surgical resection of the epileptogenic tissues. The main difficulty in the treatment is the localization of the tissue responsible for the generation and spread of the seizure activity with current technology [1].

A new optical imaging method called intrinsic imaging of optical signals (IIOS) for the mapping of the neocortical epileptic tissues in patients has been applied, which can provide high-resolution maps of the brain areas in human beings [1][2]. Applying the IIOS to collect the high resolution brain image data in the patient for a period of time, neuroscientists can monitor the change of the blood volume or blood oxygenation and try to see which parts of the brain are responsible for the epileptogenic activities. IIOS measures activity-evoked changes of the blood volume according to the brain imaging data of one particular time spot. The current method used by neuroscientists is to choose a small region of the brain and take the average of the values in the region they chose to create a univariate time series data. One of the problems for the approach is that the average for the chosen region at one time spot is dependent on the similarity of the data in that region. It is not accurate to take the average if there are not enough similar values in the region. Therefore, our specific research goal is to describe and quantify the similarity of the values in the region chosen, and furthermore, to study whether the similarity will change with respect to time.

We focus on the spatial autocorrelation [3] of the chosen region (mostly with brain tissues) of the 2D brain image data. There are many methods for studying the spatial autocorrelation. In our project, we used Moran’s I coefficient to quantify the spatial autocorrelation of the 2D data. Moran’s I coefficient is a measurement of the correlation between the value of one variable at one location and the values in the neighboring locations. Moreover, we apply the autocorrelation function in the 2D spatial data. By those two methods, we are able to quantify the similarity of the spatial data.

Now we describe how the draft is organized. In section 2, we demonstrate how the brain image data is collected and the available data we have. In section 3, we focus on the methodology to study the spatial autocorrelation: Moran’s I coefficient and 2D autocorrelation function, including the basic theories and examples. In section 4, it is the simulation to get the criteria to choose the similar levels. In section 5, we obtain the results and make the conclusion (including further work which will be done). Section 6 is the reference.

2. Experiment and Data

It is known that the optical scattering and absorption properties of brain tissue are dynamic and vary as a function of neuronal activity. These optical changes evoked by neuronal activity are known as “intrinsic optical signal” (IOSs). The optical changes can provide high-resolution maps of pathologic brain areas in humans. The IOS in brain tissue is thought to be generated in large part by changes in blood volume and blood oxygenation. By selecting the appropriate optical wavelengths, IOS-imaging (IIOS) is capable of monitoring each of these physiologic components (i.e., blood volume vs. blood oxygenation) independently. [1]

To interpret IIOS data, it is necessary to consider the optical absorbance spectra of deoxygenated hemoglobin (Hb) and HbO2 optical absorbance. Isopiestic points present ideal wavelengths to measure blood-volume changes independent of blood-oxygenation changes. Since Hb and HbO2 have identical values at isobestic points, wavelengths representing isobestic points are located where their differences in light absorption vanish and wavelengths at which Hb and HbO2 are maximally distinguishable. In our experiment, 535nm wavelength light is sensitive to blood-volume changes and independent of blood-oxygenation changes. 660nm wavelength light is sensitive to blood oxygenation changes.

To illuminate the cortical surface, four fiberoptic lights regulated by a stable DC power supply are filtered with bandpass filters (<10nm) at the following wavelengths: 535nm (specific for blood-volume changes) and 660nm (specific for blood-oxygenation changes).

In the experiment, several bipolar stimulating electrodes are placed on the cortical surface of the patients to elicit epileptogenic activity through current. Simulation currents are initially tested at a low setting and gradually increased until a current is found that is just sufficient to consistently elicit an episode of afterdischarge activity. In this way, stimulation currents are found that allow for imaging the cortex in response to stimuli that elicit epileptiform activity. The cortex is illuminated with either 535nm or 660nm light. Images are acquired with a high-quality, cooled, digital CCD camera with a dynamic range of 16 bits. Images were acquired at a rate 0.04s/image up to 16 seconds.

With the IIOS method introduced, we present some example data and get one time point data plot. The data plot in Figure 2.1 contains 512*512 pixels representing values of blood volume at one time spot. The color bar shows different levels of the blood volume. The cortex region is illuminated with the 535nm wavelength light which is sensitive to changes of blood volume. From the graph, the dark red regions with numbers are bipolar electrodes (around level 4000). The dark regions without numbers are tissues which are thought to be activity-evoked. These dark pixels show great values in blood volume (around the level 2000-3000). They are the regions we would like to focus our study on. The blue regions have smaller blood volume changes (around level 1000). Most of these parts are vessels and grey matter tissues that are not activity-evoked. They aren’t considered as pathologic regions.

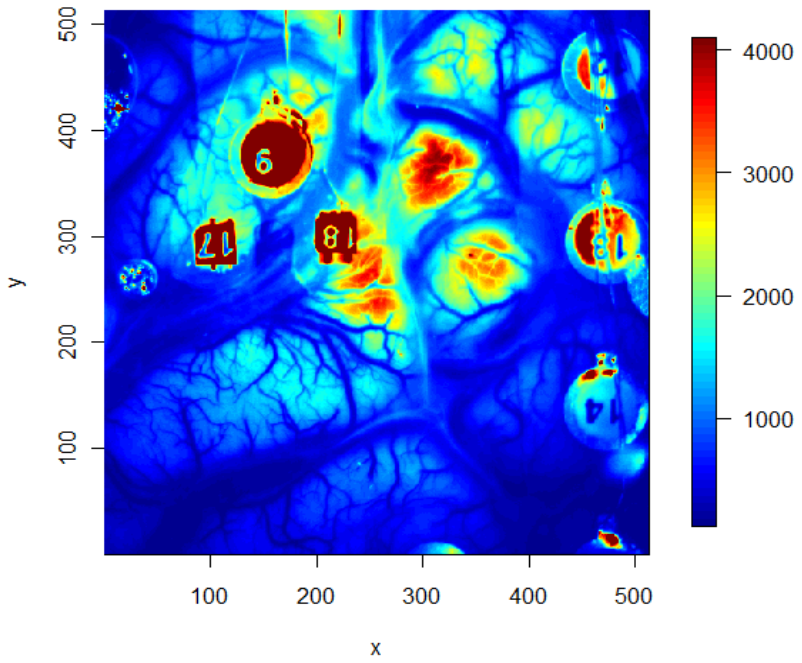

Figure 2.1: the real data for 512*512 pixels at one time spot

In our project, we chose the potentially pathologic regions to study. After comparing results of 81*81, 54*54 and 27*27 regions, we found that 27*27 is a suitable region to investigate. According to the distribution of the activity-evoked pixels in the region, generally they are unimodal structure (e.g. Figure 2.2(a)(b)) or multimodal structure (e.g. Figure 2.2(c)). We first study 27*27 pixels with unimldal structure, and later multimodal structure.

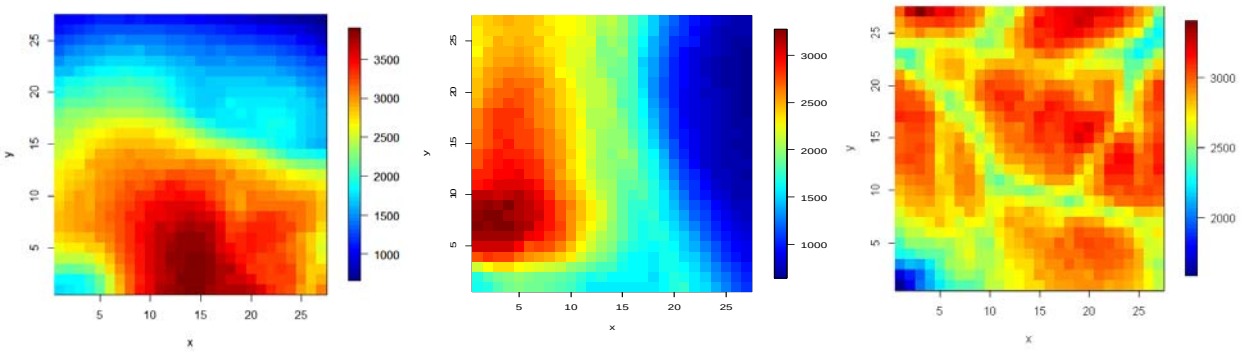

(a) (b) (c)

Figure 2.2: Structure types of 27*27 pixels. (a) (b) unimodal structure (c) multimodal structure

3. Methodology

Briefly speaking, the spatial autocorrelation is a correlation of a variable with itself through space, which measures the similarity among the spatial distribution of a variable. Specifically, positive spatial autocorrelation shows that similar values are close to each other while negative spatial autocorrelation demonstrates the dissimilar values appear close to each other. Once the spatial autocorrelation concept is established, we need to quantify the spatial autocorrelation and then test hypotheses about it. Classically, the most common used quantitative index is the Moran's I [3][4][5][6][8][10]. Additionally, inspired by the autocorrelation function for time series data [7][9], we create two dimensional autocorrelation function (2D ACF) to be another quantitative index.

3.1 Moran's I

3.1.1 Definition of Moran's I

Moran's I is structured like the Pearson product–moment correlation coefficient.

$$I = \frac{\sum_{i=1}^{n}\sum_{j=1}^{n} w_{ij}(x_i - \bar{x})(x_j - \bar{x}) / \sum_{i=1}^{n}\sum_{j=1}^{n} w_{ij}}{\sqrt{\frac{\sum_{i=1}^{n}(x_i - \bar{x})^2}{n}}\sqrt{\frac{\sum_{i=1}^{n}(x_i - \bar{x})^2}{n}}}$$

Where n is the total number of observations in a region

x_i is the variable value at a particular location i

$\bar{x}$ is the mean of the variable

w_{ij} is called a spatial weight:

$$w_{ij} = \begin{cases} 1 & \text{location i and j are neighbours} \\ 0 & \text{otherwise} \end{cases}$$

While Pearson product–moment correlation is a relationship between two variables, Moran's I involves only one variable. It is correlation between the value of variable x and the "spatial neighbor" value of x formed by averaging all the values of the neighboring locations.

3.1.2 Meaning of Moran's I and hypothesis testing

The values of Moran's I vary between -1 to 1. The values of Moran's I close to +1 indicate high positive spatial autocorrelation (the neighboring areas are more alike); the values of Moran's I around 0 indicate no spatial autocorrelation (the neighboring areas are randomly and independently distributed.); the values of Moran's I close to -1 indicate high negative spatial autocorrelation (the neighboring areas are unlike). Then Moran's I can be considered as a measurement of similarity: the larger the Moran's I, the higher the similarity level. Under a fixed neighboring definition (see section 3.1.4), one region has a single value of Moran's I. By definition, this single value of Moran's I is kind of "average similarity" between pixels and their neighbors for all pixels in the region.

The hypothesis test concerning similarity is called Moran test, which is based on the normal frequency distribution with $Z-\text{score}$:

$$Z = \frac{I - E(I)}{S_{error}(I)}$$

where: I is the calculated value for Moran's I from the sample.

$E(I) = -1/(n-1)$ is the expected value of I if the samples are chosen randomly.

$S_{error}(I)$ is the standard error of I.

H_0: Moran's I = 0 (no spatial autocorrelation)

H_a: Moran's I > 0 (positive spatial autocorrelation exists, certain similarity)

It is important to emphasize that the positive Moran's I is the case we are interested in. Therefore, from now on, we refer the null and negative Moran's I to "no spatial autocorrelation".

3.1.3 Illustrative examples

As an illustration, consider the two regions in Figure 3.1. We calculate the Moran's I and do Moran test for both regions. The results are given in Table 3.1.

(a) region 1 (b) region 2

Figure 3.1: Two regions used to illustrate Moran's I. (a) region 1: neighboring areas are randomly distributed or unlike. (b) region 2: neighboring areas are alike.

Table 3.1: Moran's I and Moran test for two regions in **Figure 3.1**

	Moran's I	P-value
Region 1	-0.14871795	0.8328
Region 2	0.67147436	<6.315e-11

For region 1: the Moran's I = -0.14871795 and p-value = 0.8328 illustrate that, using 5% significant level, region 1 has no spatial autocorrelation, supporting the common belief that the neighboring areas are not similar in region 1.

For region 2: Using 5% significant level, region 2 has certain positive spatial autocorrelation, supporting the common belief that the neighboring areas are similar in region 2. This similarity in the neighboring areas is measured by Moran's I value 0.67147436.

3.1.4 Refined Moran's I

There is one important element in definition of Moran's I: neighbor. Classically, three types of neighbor definition [4] are given in Figure 3.2.

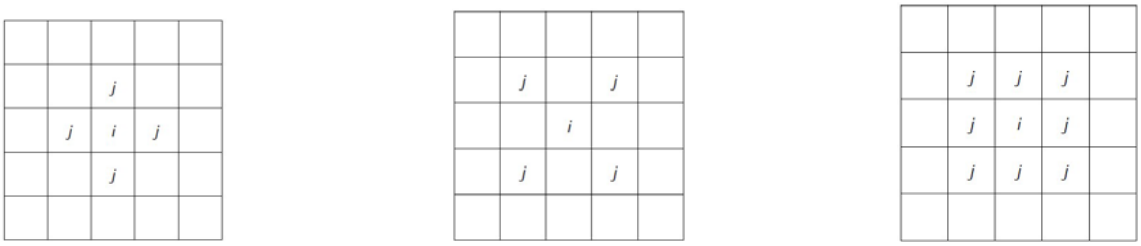

(a) Rook's case (b) Bishop's case (c) Queen's case

Figure 3.2: Three types of neighbor definition. (a) Rook's case: pixels sharing a common edge are considered neighboring. (b) Bishop's case: pixels sharing a common vertex. (c) Queen's case: pixels sharing a common edge or common vertex.

Based on the three types of neighbor definition in Figure 3.2, the classical Moran's I only quantifies the similarity between immediate neighbors. In order to measure the similarity between neighbors who are not immediate neighbors, we refine the definition of neighbor and name the modified Moran's I based on the new neighbor definition as "Refined Moran's I".

The refined definition of neighbor is: for a pixel, its neighbors are all pixels within the circle of radius r. Under this neighboring definition, Moran's I is the average similarity among all circles with radius r in the investigated region. For a series of r, we compute the corresponding Moran's I. Then we can draw the plot represents the relationship between Moran's I and radius r. This plot will be a function plot of Moran's I with respect to radius r.

3.2 2D ACF

One of the contributions of this project is that we create a new method named Two-dimension Autocorrelation Function (2D ACF) to study the spatial autocorrelation. The basic idea of 2D ACF is inspirited by autocorrelation function for time series data [7][9].

3.2.1 Definition of 2D ACF

Figure 3.3 below is used to illustrate the definition of 2D ACF. For a specific pixel, e.g. x_1, we define the Lag-1 pixels of x_1 are the red color pixels around x_1, i.e., { y_1, y_2, … , y_8}; the Lag-2 pixels of x1 are the blue pixels outside, i.e., { z_1, z_2, … , z_{16}}.

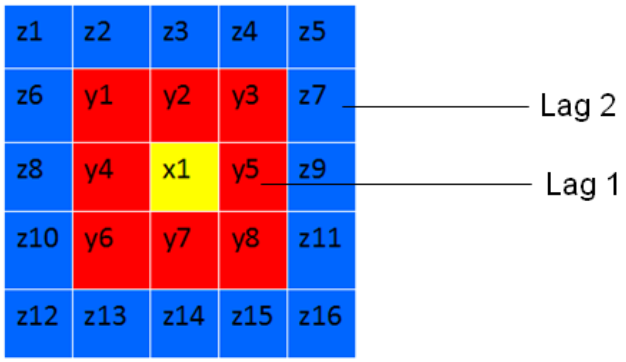

Figure 3.3: illustration 2D-Acf definition

Define a 1×8 vector $X = (x_1, x_1, ..., x_1)$ and a 1×8 vector $Y = (y_1, y_2, ..., y_8)$. The Lag-1 two-dimension autocorrelation of x_1 is the correlation between X and Y. Similarly, define a 1×16 vector $X = (x_1, x_1, ..., x_1)$ and a 1×16 vector $Z = (z_1, z_2, ..., z_{16})$. The Lag-2 two-dimension autocorrelation of x_1 is the correlation between X and Z.

For the whole region in Figure 3.3, if we combine all the X vectors for all pixels into one vector $\tilde{X} = (x_1, x_1, ..., x_1, y_1,..., y_1,..., z_{16},..., z_{16})$ and combine all the Y vectors (Lag 1 pixels) for all pixels into one vector $\tilde{Y} = (y_1, ..., y_8, z_1, z_2, z_3, z_6, y_2, z_8, y_4, x_1, ..., y_8, z_{11}, z_{15})$ (follow the same combination order with $\tilde{X}$), the Lag-1 two-dimension autocorrelation of this region is defined to be the correlation between $\tilde{X}$ and $\tilde{Y}$. Similarly, if we combine all Z vectors (Lag 2 pixels) for all pixels into one vector $\tilde{Z}$, the Lag-2 two-dimension autocorrelation of this region is defined to be the correlation between $\tilde{X}$ and $\tilde{Z}$.

Therefore, we define the Lag- N two-dimension autocorrelation of a region by the correlation between the original pixels vector and the Lag N pixels vector. Given a finite number N, Lag-N two-dimension autocorrelation is a single value. Then the function of Lag-N two-dimension autocorrelation with respect to N is called 2D ACF.

3.2.2 Meaning of 2D ACF

Since the 2D ACF value is a correlation value, it varies between -1 to 1. Similar to Moran's I, the values of 2D ACF close to +1 indicate high positive spatial autocorrelation (the neighboring areas are more alike); the values of 2D ACF around 0 indicate no spatial autocorrelation (the neighboring areas are randomly and independently distributed.); the values of 2D ACF close to -1

indicate high negative spatial autocorrelation (the neighboring areas are unlike). 2D ACF is the average similarity among all squares with edge length 2*N+1 in the investigated region, where N is lag number.

3.2.3 Illustrative examples

As an illustration, consider the two regions in Figure 3.1. We calculate the 2D ACF for both regions. The results are given in Figure 3.4 and Table 3.2.

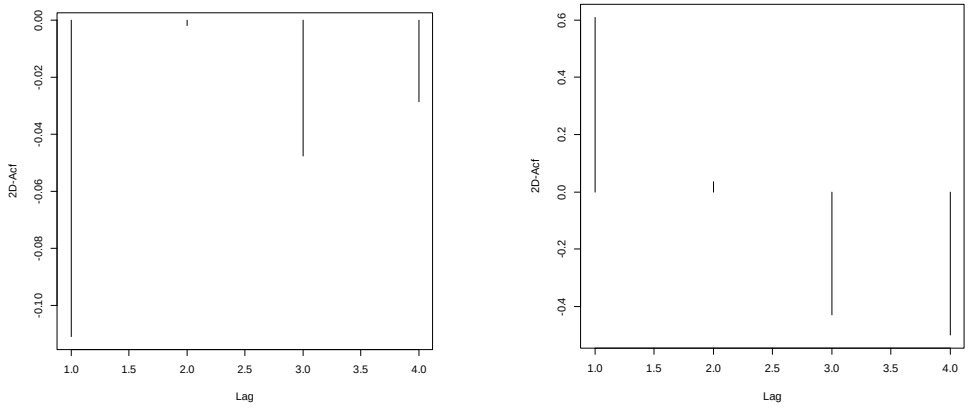

(a) Region 1 (b) Region 2

Figure 3.4: 2D ACF plot for two regions in Figure 3.1.(a) 2D ACF plot for region 1. (b) 2D ACF plot for region 2.

Table 3.2: 2D-Acf value for two regions in Figure 3.1

Lag N		1	2	3	4
2D ACF	Region 1	-0.1111111	-0.00173913	-0.04761905	-0.02857143
	Region 2	0.6099071	0.03496503	-0.4285714	-0.5

For region 1: the 2D ACF values are negative (near 0) for all lag number, meaning that region 1 has no (or slightly negative) spatial autocorrelation. This conclusion is consistent with the conclusion from Moran's I, all supporting the common belief that, averagely, all pixels and their lag-N pixels are not similar in region 1.

For region 2: the 2D ACF value for lag-1 is positive number = 0.6099071 > 0.5, meaning that region 2 has positive spatial autocorrelation. This conclusion is consistent with the conclusion from Moran's I, supporting the common belief that, on average, all pixels and their lag-1 pixels are similar in region 2. In other words, all squares with edge-length 3 in region 2 have similarity, which is measured by 2D ACF value 0.6099071. Similarly, 2D ACF for lag-2 is around 0, meaning that the similarity for all pixels and their lag-2 pixels is low. 2D ACF for lag-3 and lag-4 are significantly negative, meaning that all pixels and their lag-3 and lag-4 pixels are unlike.

4. Discussion for Criteria:

After we quantify the spatial autocorrelation using refined Moran's I and 2D ACF, the next question is how to decide the criteria for choosing similarity level. One approach is to simulate a well-known data distribution whose data structure is similar to our real data, derive the refined Moran's I and 2D ACF for the simulated data, and use several standard deviations (sd.) of the simulated data to decide the criteria: high, moderate, and low similarity level.

4.1 Simulating 2D normal distribution data

In section 2, one type of data inside of some subregions has unimodal structure, e.g. Figure 2.2 (a)(b). We start by studying this type of subregion in this section. Then this method can be extended to other types in the future.

If the real objective data has unimodal structure, we simulate 2D normally distributed data to study the criteria. Additionally, the size of simulated region should coincide with the size of investigated region. Figure 4.1 is the simulated 2D normal distribution data for 27×27 pixels.

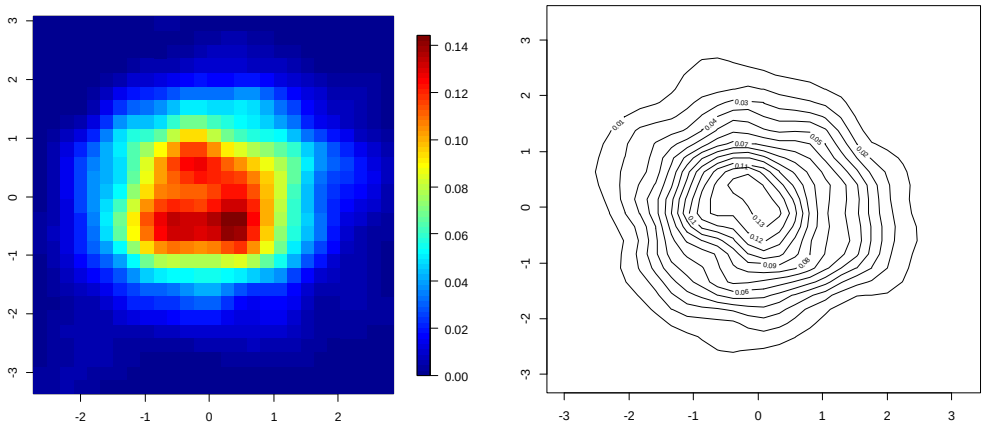

(a) data image (b) contour plot

Figure 4.1: the simulated 2D normal distribution data for 27×27 pixels.

4.2 Refined Moran's I and 2D ACF for the simulated data

For the region we simulated in Figure 4.1, we apply refined Moran's I and 2D ACF. The results are shown in Figure 4.2 and Table 4.1.

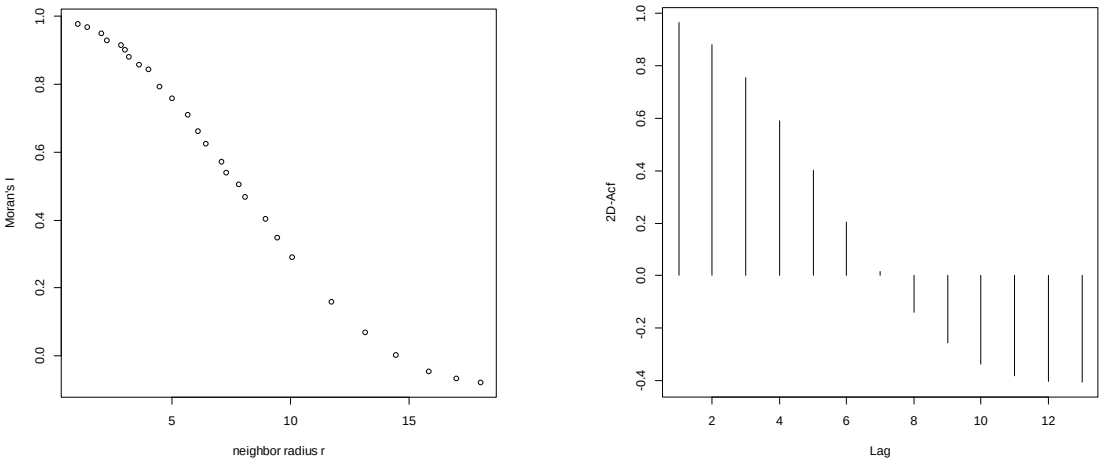

(a) Moran's I v.s. radius r (b) 2D ACF v.s. Lag number

Figure 4.2: Moran's I and 2D ACF plot for simulated region in Figure 4.1.(a) Moran's I (b) 2D ACF

Table 4.1: Moran's I and 2D ACF values for simulated region in Figure 4.1

radius	Moran's I	lag	2D ACF
1.000000	0.98	1	0.97
1.414214	0.97	2	0.88
2.000000	0.95	3	0.755
2.236068	0.93	4	0.59
2.828427	0.91	5	0.40
3.000000	0.90	6	0.20
3.162278	0.88	7	0.017
3.605551	0.86	8	-0.14
4.000000	0.84	9	-0.26
4.472136	0.79	10	-0.34
5.000000	0.76	11	-0.38
5.656854	0.71	12	-0.40
6.082763	0.66	13	-0.41
6.403124	0.625		
7.071068	0.57		
7.280110	0.54		
7.810250	0.505		
8.062258	0.47		
8.944272	0.40		
9.433981	0.35		
10.049876	0.29		
11.704700	0.16		
13.152946	0.07		
14.422205	0.004		
15.811388	-0.045		
17.000000	-0.066		
18.000000	-0.078		

4.3 Criteria for the simulated data

We define the Moran's I and 2D ACF values corresponding to 0.5sd, 1sd, and 1.5sd of the simulated data respectively to be similarity level: high, moderate, and low. From Table 4.1, we obtain the criteria, shown in Table 4.2 below.

Table 4.2: Criteria of similarity level for the simulated region in Figure 4.1.

Similarity level	Position in simulated region	Radius	Moran's I value	Lag	2D ACF value
High	0.5 sd	2	0.95	2	0.88
Moderate	1 sd	4	0.84	4	0.59
Low	1.5 sd	6	0.66	6	0.20

(We may add criteria for multimodal normal data later.)

5. Results and Discussion

In this section, we present the Moran's I and 2D ACF results for our real data, the measure of blood volume data. Figure 5.1 is one investigated region containing 27×27 pixels, a sub-region

of the real data image in Figure 2.1. Figure 5.2 shows two plots of Moran's I and 2D ACF for blood volume data in investigated region in Figure 5.1. In Figure 5.2(a), the points are denser for higher Moran's I (> 0.6) since the similarity levels we are interested in are larger than 0.6 Moran's I. (See Table 4.2)

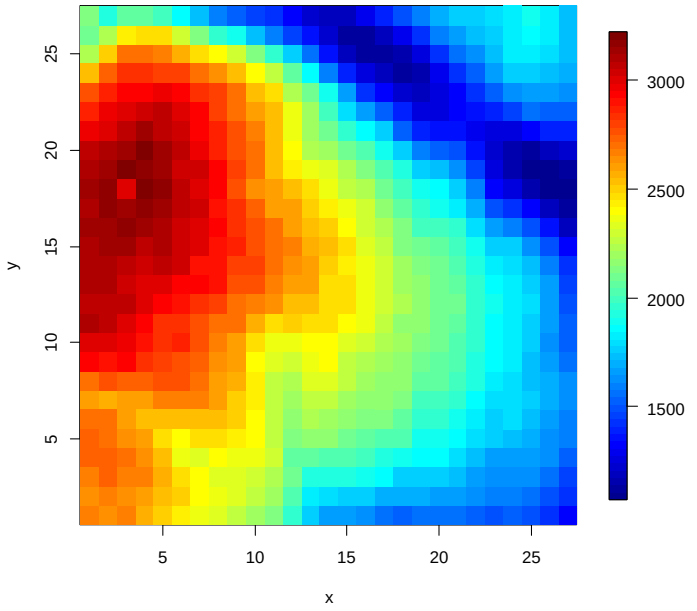

Figure 5.1: 27×27 pixels in real data image in Figure 2.1.

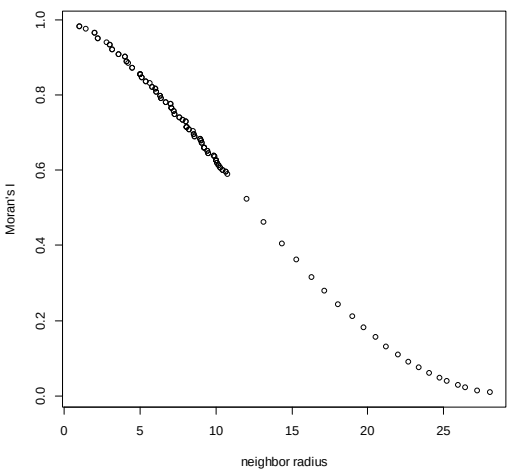

(a) Moran's I v.s. radius

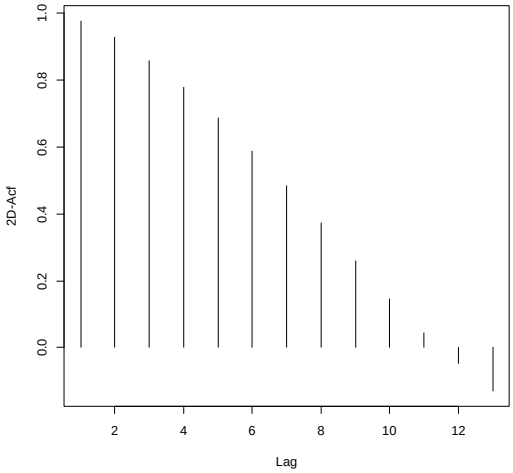

(b) 2D ACF v.s. lag

Figure 5.2: (a) Moran's I and 2D ACF plot for blood volume data region in Figure 5.1.(a) Moran's I (b) 2D ACF

Using the criteria in Table 4.2 for Moran's I and 2D ACF, Table 5.1 gives the result for the investigated region in Figure 5.1. For example, the Moran's I value for high similarity level is 0.95, the corresponding radius in plot Figure 5.2(a) is 2.236068; the 2D ACF value for high similarity level is 0.88, the corresponding lag in plot Figure 5.2(b) is 2, etc.

Table 5.1: Moran's I corresponding to radius and 2D ACF corresponding to lag for real data region in Figure 5.1.

Similarity level	Moran's I value	Radius	2D ACF value	Lag
High	0.95	2.236068	0.88	2
Moderate	0.84	5.099020	0.59	5
Low	0.66	9.055385	0.20	9

Conclusion:

Based on the results in Table 5.1, averagely speaking, all circles with radius r = 2.236068 in the investigated region have high similarity level and all squares with edge length 5 in the investigated region have high similarity level; all circles with radius r = 5.099020 in the investigated region have moderate similarity level and all squares with edge length 11 in the investigated region have moderate similarity level; all circles with radius r = 9.055385 in the investigated region have low similarity level and all squares with edge length 19 in the investigated region have low similarity level.

(We may add multimodal region result later.)

6. Reference

[1] Michael M. Haglund and Daryl W. Hochman, Optical Imaging of Epileptiform Activity in Human Neocortex, Epilepsia, 45 (Suppl.4): 43-47, 2004, Blackwell Publishing, Inc.

[2] Michael M. Haglund and Daryl W. Hochman, Imaging of Intrinsic Optical Signals in Primate Cortex during Epileptiform Activity, Epilepsia, 48 (Suppl.4): 65-74, 2007 Blackwell Publishing, Inc.

[3] D. A. Griffith, Spatial Autocorrelation 2009 Elsevier Inc.

[4] Yuri M. Zhukov, Workshop: Applied Spatial Statistics in R

[5] Spatial Autocorrelation (Moran's I) (Spatial Statistics), ESRI Developer Network.

[6] Moran's I, Wikipedia

[7] Autocorrelation, Wikipedia

[8] Spatial Autocorrelation, Arthur J.Lembo, Jr Salisbury University

[9] W.N. Venables and B. D. Ripley, Modern Applied Statistics With S

[10] Danlin Yu, Spatial Association and spatial techniques